Plasma diagnostics in large area plasma processing system

D. Leonhardt,[a] S. G. Walton, D. D. Blackwell, W. E. Amatucci, D. P. Murphy, R. F. Fernsler, and R. A. Meger
U.S. Naval Research Laboratory, Plasma Physics Division, Washington, DC 20375

(Received 9 October 2000; accepted 5 February 2001)

A series of plasma diagnostic have been carried out in our large area plasma processing system which is based on a modulated electron-beam produced plasma. These discharges were created in both electrically conducting and insulated vacuum chambers operated in 30–120 mTorr of pure gases (argon, oxygen, and nitrogen). Langmuir probes, microwave transmission, mass spectrometry, and external current sensors show robust discharges were made over fairly wide parameter ranges resulting in plasma densities of $1-4\times10^{11}$ cm^{-3} and temperature ranging from 0.2 eV for the molecular gases and 1.4 eV for argon. The effects of various experimental techniques, parameters, and contamination issues are discussed in detail. © *2001 American Vacuum Society.*
[DOI: 10.1116/1.1359554]

I. INTRODUCTION

Electron beam (*e*-beam) generated discharges have been shown to be efficient at producing high density plasmas[1] and possess characteristics favorable for materials' processing applications.[2] The previous ''large area'' work[1] emphasized reflection of *X*-band microwaves (requiring electron densities $>10^{12}$ cm^{-3}) at fairly high pressures (up to 300 mTorr) using various operating modes of hollow-cathode discharges to generate an *e*-beam. Although the *e*-beam was collimated by an external magnetic field, the mode operation was not always stable, typically having narrow operating windows. Materials' processing work[2] applied a freely expanding *e*-beam plasma as a secondary source of ionization in a reactive ion etching reactor. In this configuration, enhanced plasma densities of 10^9-10^{10} cm^{-3} were seen in the beam region but etch uniformity was low since the beam did not propagate the entire substrate length. The authors noted that accurately defining the beam geometry and extent was necessary due to the rapid variation of plasma characteristics with distance to the substrate.

In this article, we studied highly stable modes of operation of magnetically collimated *e*-beam plasmas with global measurements (microwave transmission, current sensors) as well as highly localized plasma diagnostics (Langmuir probes). Surface interactions and relative cation fluxes were also investigated in a high vacuum system via a quadrupole mass spectrometer to further diagnose such discharges *in situ* for future materials' processing applications.

II. EXPERIMENT

Electron beam produced discharges were created in a cylindrical Plexiglas chamber (38 cm in diameter and 50 cm tall) and a cylindrical aluminum vessel (50 cfm in diameter and 65 cm tall). For the Plexiglas chamber, a (45 cm) rotary vane pump provided an ultimate base pressure of ~4 mTorr and manual variable leak valve permitted good control of gas flow to vary chamber operating pressure. The aluminum high vacuum system was pumped by a 150 l/s tubomolecular pump, and provide based pressures in the 8×10^{-6} to 1.5×10^{-5} Torr range. Gas flow in this chamber was controlled by throttling the turbo pump via a low-conductance tube and introducing gases through mass flow controller units (MKS 1179 Series). The purity of gases used in these experiments were 99.999% argon and >99.8% nitrogen and oxygen. Convectron® and/or Pirani-type vacuum gauges were used to determine operating pressures and the reported readings have been corrected for the particular gas type.

The electron beam was generated by a hollow cathode (as in Ref. 1) consisting of a 1 cm wide channel in 2.5 cm diam brass rod stock. The channel was approximately 1.5 cm deep and 22 cm long. A 1.6 mm thick teflon sheet and ground shield cover the inactive cathode surfaces to suppress unwanted electrical breakdowns. The electron beam generated by the cathode is physically skimmed by a stainless steel shim stock anode containing a 1×20 cm slot aligned with the cathode hollow and placed ~5 cm downstream. A second anode, placed ~25 cm downstream of the first acts as the beam dump. Both anodes are grounded outside of the chamber so that the currents collected on them can be monitored with Pearson coils. The beam between the anodes is centered in a pair of 50 cm diam. Helmholtz coils, which provides an axial magnetic field with uniformity better than 2% over the discharge area. Figure 1 shows the geometric layout of the cathode and anodes. The resultant *e*-beam sheet is therefore defined by the slotted anode (1 cm×20 cm) and the distance $(\sim25\ cm)$[3] to the beam dump anode. A large impedance voltage divider is connected in parallel with the cathode/anode on the vacuum chamber to monitor the voltage drop across the cathode and beam dump anode and to infer a relative plasma impedance. High voltage pulses (2.5 kV) are generated via a homemade unit[4] based on insulated gate bipolar transistor technology. Pulses used here are 500–1000 μs in length at repetition rates of 1–50 Hz. While much larger duty factors (>50%) are possible without loss of plasma stability, data collection in these experiments was

[a]Electronic mail: darrin@ccf.nrl.navy.mil

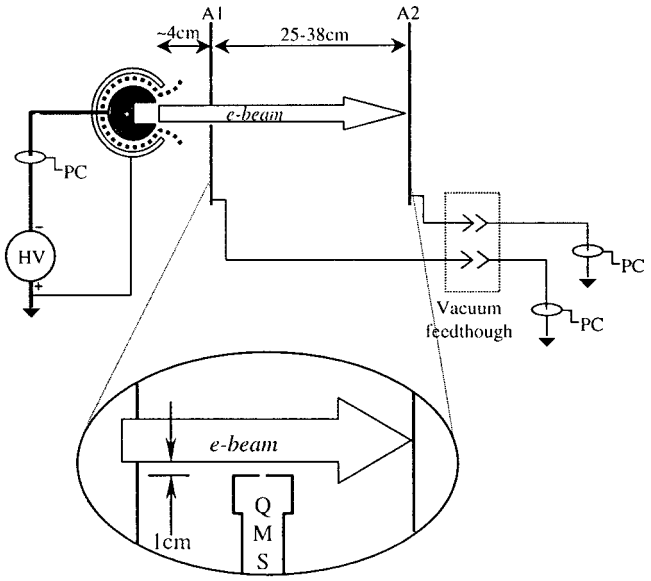

FIG. 1. Cross-sectional layout of hollow cathode and anodes used to generate electron beam and subsequent electron beam generated discharge. The hollow cathode is drawn in solid black, teflon insulation by dashed line. A1 and A2 are the slotted and beam dump anodes, respectively. Pearson coils are labeled PC. Position of mass spectrometer orifice with respect to the plasma is shown separately in detail for clarity.

dictated by human response times.

Microwave transmission measurements were carried out in the Plexiglas chamber using 20 dB horns straddling the plasma sheet outside the chamber. A Hewlett-Packard frequency synthesizer (1–25 GHz) was used as the microwave signal source. The microwave signal is amplitude modulated at ~20 kHz to clearly identify baseline levels of the signal during the plasma modulation.

Due to the rough vacuum environment in the Plexiglas chamber, contamination of the Langmuir probe resulted in irreproducible data. We found it necessary to heat the probe externally[5] to achieve consistent data in this environment. Thus, single Langmuir probe construction consisted of a 0.25 mm (10 mil) thoriated tungsten wire protruding 2 mm out of an alumina tube. The aluminum tube was 0.156 cm in diameter with four 0.381 mm (15 mil) bores. A 4 cm ''hairpin'' of nichrome wire was wound around the alumina tube and was used to heat the probe tip locally. Ceramic paste coated the heater element and contact wires to shield them from the plasma. A type *K* thermocouple was also inserted through two of the bores to monitor the probe's temperature. For all but the last 4 in. of the probe, all wires and connections were enclosed in a grounded tube. It was found that if the probe temperature was kept at around 500 °C, reproducible results could be obtained with this system. The probe bias voltage was provided by a potentiometer connected to gel cell batteries, which were checked for better than 10 μs time response and extremely low noise. Probe currents during and after the pulse were recorded on a digital oscilloscope.

An emissive probe was inserted into the aluminum chamber to more accurately identify the plasma potential and eliminate any systematic errors within the single probe measurements. Similar ceramic and tungsten materials were used for this probe as well. The tungsten wire[6] was bent into a hairpin geometry with a radius of curvature of ~1 mm. This wire was press fit into ceramic tubing with 18 gauge copper wire which ran to a high current vacuum feedthrough. Emission of the probe was controlled by a (floating) dc power supply operated in constant current mode. Typical probe current–voltage (*I–V*) traces were obtained by applying a bias voltage to the probe and monitoring the collection current though the probe by measuring the voltage across a standard carbon resistor, as in the single probe measurements. Data were recorded using boxcar averagers (Stanford Research Systems SR250) with 1–10 μs sample gates positioned during the *e*-beam, then 50 and 100 μs after the beam had been terminated.

Mass spectrometry was carried out in the aluminum high vacuum chamber using a quadrupole mass analyzer (Hiden EQP300). The mass spectrometer was differentially pumped and sampled species through a 100 μm orifice. The orifice was grounded and positioned parallel to the *e*-beam, simulating a wafer chuck for materials' processing applications 1 cm away from the edge of the *e*-beam (see Fig. 1 detail). The base pressure was $\sim 1\times10^{-8}$ Torr which increased to $\leqslant 2\times10^{-6}$ Torr when the plasma chamber pressure was 100 mTorr. The body of the mass spectrometer was constantly baked to minimize background gas interferences. Further details are available in Ref. 7.

III. DATA

A. Oxygen and nitrogen

With a 2.5 keV *e*-beam, electron beam currents[8] of ~5 mA/cm^2 were readily produced by the cathode, over a large pressure range (30–120 mTorr) of oxygen or nitrogen and magnetic field (120–300 G). Figure 2 shows N_2 discharge parameters as measured by the external sensors (Pearson coils and microwave transmission) in the Plexiglas chamber. Corresponding raw data from the time-resolved Langmuir probe measurements are shown in Fig. 3 for the analogous O_2 discharge. The probe is heated to 500 °C and positioned in the center of the discharge. Emissive probe data taken in the high vacuum chamber are shown in Fig. 4 for the same N_2 discharge. All nonspatially resolved probe measurements shown are taken at the center of the discharge. Emissive probe measurements were not achievable in an O_2 working gas.

B. Argon

The 2.5 kV *e*-beam produced beam currents of ~20 mA/cm^2 as measured by the external sensors similar to N_2 and O_2. Under the same operating conditions, the argon discharge had a higher plasma density, attenuating 7.5 GHz microwaves completely. In certain pressure and magnetic field regimes, much more beam current was produced by the cathode, which led to a significant drop in anode–cathode voltage. These higher current/lower impedance modes possessed significantly higher electron densities but were un-

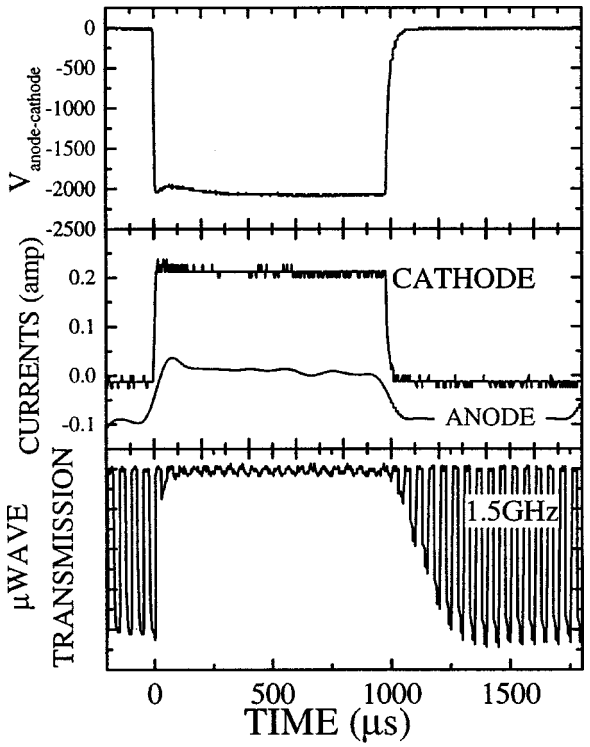

FIG. 2. External plasma diagnostics (voltage, cathode current, anode current, and microwave transmission) for N_2 discharge at 75 mTorr and 150 G. The anode current is offset for clarity. Complete attenuation of the 1.5 GHz microwaves implies (see Ref. 9) a plasmas density of $>5\times10^{10}$ cm^{-3}. Electron beam pulsewidth is 1 ms.

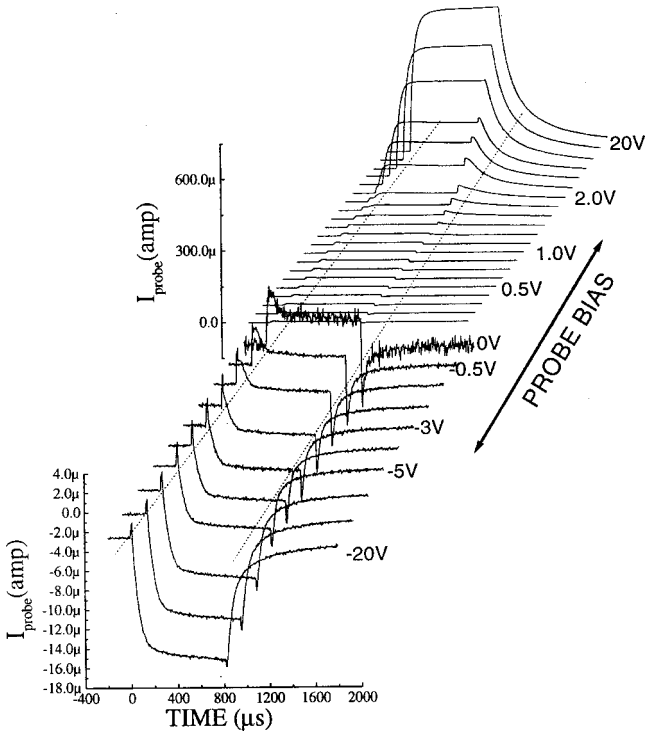

FIG. 3. Single Langmuir probe currents of various probe bias voltages before, during, and after the *e*-beam produced O_2 plasma. Probe is heated to 500 °C via the external heater and the plasma conditions are the same as in Fig. 2, at a 800 μs pulsewidth.

stable in time and therefore not studied extensively. Characteristic probes *I–V* traces from the Plexiglas chamber are shown in Fig. 5.

IV. RESULTS

A. Oxygen and nitrogen

Oxygen and nitrogen *e*-beam generated discharges show similar characteristics at the conditions investigated here. Both gases formed plasmas with densities from 1×10^{10} to 5×10^{11} cm^{-3} according to probe and microwave cutoff[9] measurements. Microwave cutoff measurements are provided as a lower bound and sanity check on the probe data. Probe measurements in the Plexiglas chamber were analyzed using a two temperature fitting routine[10] which assumes Maxwellian electron distributions. The current in the ion saturation region is assumed to be proportional to $(-V)^{1/2}$, then coupled to two electron saturation regions with $\exp(-V/T_e)$ dependencies. Variables of the fit are adjusted to minimize the discrepancy between the fit and the data. Two-temperature distributions down to 0.10 eV have been clearly seen using this particular algorithm, thus we believe it to be well suited for this application. Spatial profiles for the resultant densities and electron temperatures for N_2 discharges are given in Figs. 6 and 7. Figure 6 shows densities and temperatures along the electron beam axis. Figure 7(a) shows the ion saturation current measured with a probe bias of -20 V, and Fig. 7(b) shows the electron temperature across the plasma sheet. Oxygen data showed very similar results, giving slightly lower plasma densities (2.5×10^{11} cm^{-3}) and temperatures ($\sim$0.32 eV). Temporally resolved probe data are shown in Fig. 8 for the same N_2 discharge conditions. Oxygen discharges also show similar rapid stabilization.

Translation of the cathode from the Plexiglas (insulating) chamber to the aluminum (conducting) chamber showed no appreciable effect on the discharge conditions as measured by the external sensors and the two probe techniques. (As mentioned earlier, emissive probe measurements were only

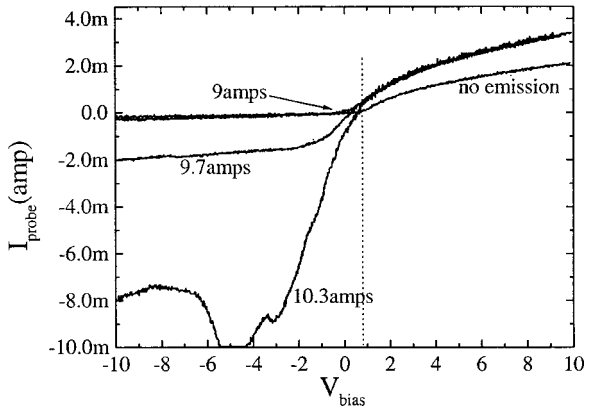

FIG. 4. Emissive probe measurements from the high vacuum chamber for the same N_2 discharge. Emission is labeled by the dc current flowing through the probe. Plasma potential as identified by strong emission curve is given by dotted line.

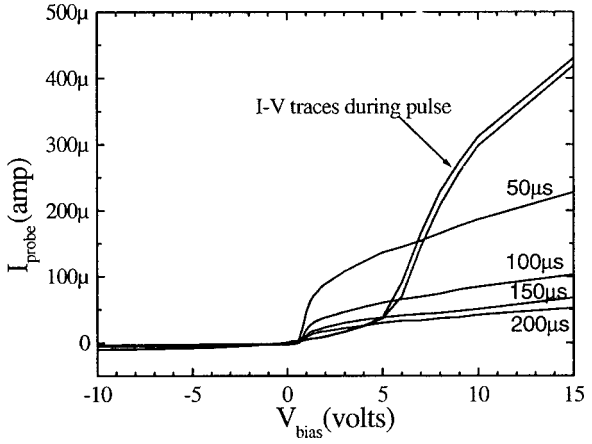

FIG. 5. Characteistic *I–V* plots from argon discharge in Plexiglas chamber using heated Langmuir probe. Postpulse curves are labeled according to their time after the plasma pulse.

carried out in N_2.) The impetus for carrying out the emissive probe measurements under higher vacuum was to substantiate the data analysis in the poorer based pressure chamber. These details are discussed in a subsequent section. The fluxes of ions detected by the mass spectrometer showed O^+ to be the dominant ion near the electron beam, with a O^+/O_2^+ flux ratio of 2:1.

B. Argon

Probe data in the Plexiglas chamber shows electron temperatures of ~1.2 eV during the *e*-beam and a rapid cooling once the *e*-beam is turned off. Plasma electron densities were $\sim 3\times 10^{11}$ cm^{-3} and also dropped rapidly once the *e*-beam was turned off, which agrees well with the microwave cutoff data. The plasma potential from these measurements was ~3–5 V. A time-resolved data plot of n_e and T_e is shown in Fig. 9. Plasma potential and temperature measurements from the emissive probe in aluminum chamber were both slightly lower, typically ~2–3 V and 1 eV during the *e*-beam and cooled more slowly once the *e*-beam was turned off. During the beam, the dominant ion flux in the mass spectrometer was atomic ions (Ar^+).

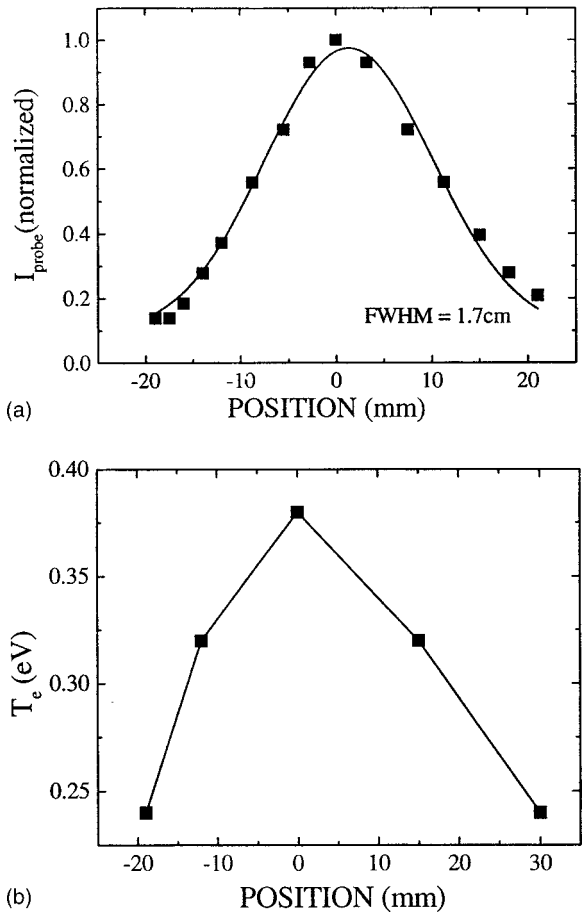

FIG. 7. (a) Ion saturation current measured with a probe bias of −20 V and (b) electron density measurements while the probe traverses the plasma sheet for the N_2 discharge shown in Fig. 2.

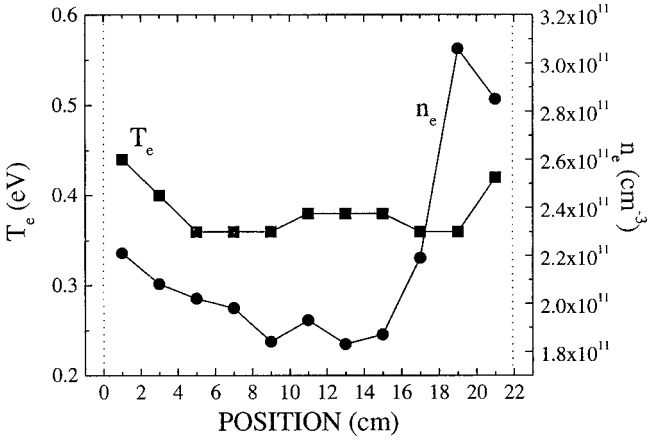

FIG. 6. Electron densities and temperatures along the electron beam axis for the N_2 discharge shown in Fig. 2. Dotted lines show the positions of the two anodes (the *e*-beam travels from left to right).

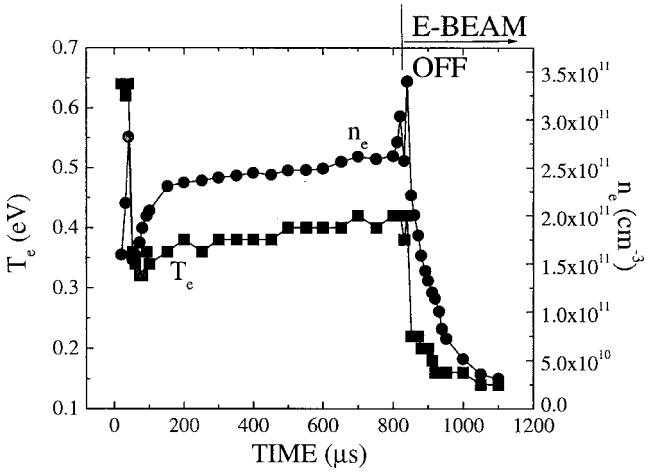

FIG. 8. Temporally resolved single probe data for the N_2 discharge shown in Fig. 2.

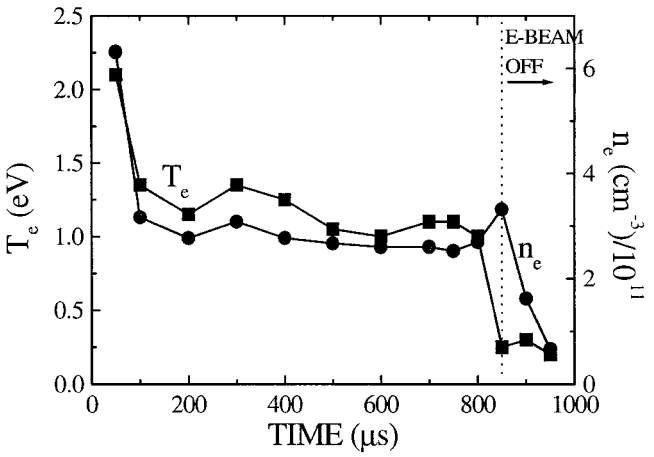

FIG. 9. Temporally resolved argon plasma electron densities and temperatures measured in Plexiglas chamber at different times during and after the electron beam, for the argon discharge shown in Fig. 5.

V. DISCUSSION

A. Oxygen and nitrogen

The strong similarities in the O_2 and N_2 discharges show that *e*-beam ionization is fairly independent of background gas. Erratic probe analyses in the (rough vacuum) Plexiglas chamber (especially in argon, see below) prompted the independent measurement of the plasma potentials via the emissive probe in the cleaner high vacuum aluminum chamber. As seen in Figs. 3 and 5, the probe *I–V* traces obtained in the Plexiglas chamber did not show a clear leveling out of the electron saturation region and thus provided poor identification of the plasma potential. Best fits to the Plexiglas chamber experimental data were achieved by forcing the plasma potential to be lower than indicated by typical first derivative ($dI_{\text{probe}}/dV_{\text{bias}}$) techniques. Excellent fits were achieved when the data were analyzed in this manner, however an independent test was still necessary to corroborate these results. The emissive probe data in the high vacuum system indeed showed similar results (see Fig. 4). A nonemissive probe trace (''no emission'' curve in Fig. 4) showed a shifted *I–V* curve, whereas when the probe was pushed even slightly emissive (9 A curve), the probe *I–V* trace shifted to a lower plasma potential and remained there through more emissive states (9.7 A and 10.3 A curves). Plasma potentials identified either from analyzing the slightly emissive curve or taking $V_{\text{float}}=V_{\text{plasma}}$ (dotted line in Fig. 4) for the extreme emission curve agreed well with the plasma potentials (and electron temperatures) from the cruder probe measurements in the Plexiglas chamber. These trends seen in the emissive probe were consistent regardless of the previous probe operation—a probe ''cleaned'' by running high currents through it gave the same ''no emission'' curve as a probe which had been cycled through 100 emission cycles. Hence, the probe surface ''contamination'' does not depend on *in situ* or *ex situ* surface preparations; the chamber base pressure of $\sim 1\times 10^{-5}$ Torr deposits 10 monolayers of oxygen, water, etc. every second, which must be constantly burned off to get accurate plasma potential identification.

The fact that both types of probe measurements fit well to two-temperature distributions demonstrates that the actual bulk electron distribution is non-Maxwellian. We expect cold distributions from *e*-beam generated plasmas created in molecular gases because ionization of the plasma comes from the beam and ionization by the plasma electrons is negligible. Thus, heating of plasma electrons is generally absent, except as byproducts of the ionizing collisions. [In typical inductively coupled plasma (ICP) or glow discharges, electron temperatures are high because the plasma electrons must be hot enough to ionize the background gas.] In molecular gases, the primary plasma electron temperature from *e*-beam produced plasma is especially low because of the large sea of inelastic levels that rapidly cools the plasma electrons.

From the data fitting routine, very cold ($\sim$0.35 eV in N_2 and $\sim$0.25 eV in O_2) electrons were measured with a second population consistently lower in density (by a factor of 2–10 and higher temperature (factor of 5–10). The dependence of this second population could be very erratic. Initially, its existence was attributed to the probe's response to the high energy electron beam. However, the beam current in the probe is well below all of the probe current measured and there was no spatial dependence associated with the geometric profile of the *e*-beam. Actually the two-temperature Maxwellian fit provides a mathematical breakdown of the non-Maxwellian bulk electron distribution. The mean electron temperature from two Maxwellians is actually give by $T_e=n_1T_{e1}/(n_1+n_2)+n_2T_{e2}/(n_1+n_2)\approx T_{e1}+(n_2/n_1)T_{e2}$. Considering a worse case where $n_1\sim 2n_2$ and $T_{e1}\sim T_{e2}/10$, $T_e\sim 4T_{e1}$. This mean temperature for the bulk distribution is indeed still very low, 1–2 eV, especially when compared to the other [non-Maxwellian] high density plasma discharges. While determining the electron energy distribution function (eedf) is not possible with the present data[11] the well defined, consistently low plasma potentials ($\sim$1 V) also indicate that the bulk T_e is indeed low.

Secondary electrons produced from *e*-beam ionizations can indeed be highly energetic initially, with a mean energy roughly one-half the ionization energy of the gas. If this high energy contribution to the actual eedf was substantial, the lower energy portion would compensate to keep thermal ionization small, driving the eedf even more non-Maxwellian. Thus, the second population generated by the two temperature fitting routine provides more of a degree of perturbation on an ideal Maxwellian eedf.

In these molecular gases, it is believed that the plasma decay or afterglow is dominated by electron–ion recombination. In that case, after the electron beam turns off, the plasma density decays from its density at the end of the pulse $n(0)$ according to $dn_e/dt=-\beta n_e^2$, where β is the recombination coefficient and electrons are the only negative charge carriers.[12] Solving this equation, we see that the ion density varies as $n(t)=n(0)/[1+\beta n(0)t]$, where t is the time after the pulse. As a check of this decay mechanism, $1/n_e$ from

Fig. 8 in the N_2 afterglow was plotted and fit to a straight line to derive an experimental recombination coefficient. This fit yields $\beta = 8.1 \times 10^{-8}$ cm^3/s for the initial decay. In N_2 the recombination coefficient varies as[13] $\beta = 4.3 \times 10^{-8} \times [T_e]^{-0.39}$, which when equated to our experimental value, gives an afterglow plasma temperature of 0.19 eV, in good agreement with the data in Fig. 8. Because the plasma temperature decreases with time, a perfect fit is not obtained over the entire range of the decay. While this result is somewhat fortuitous, given the weak temperature dependence of the recombination coefficient, the low electron temperatures ($\leqslant$1 eV) measured nevertheless support the plasmas decay mechanism. A similar analysis in the O_2 discharge (using[14] $\beta = 2.4 \times 10^{-8} \times [T_e]^{-0.5}$) results in the same afterglow temperature, which is slightly higher than the measured 0.15 eV temperature derived from probe measurements.

B. Argon

Again, the strong similarities in the molecular and noble gas discharges show that *e*-beam ionization is fairly independent of background gas. As alluded to earlier, the erratic behavior seen in the probe data from the Plexiglas chamber prompted independent measurements of plasma potentials in the cleaner aluminum vacuum chamber with an emissive probe. The emissive probe gave a more distinct identification of the plasma potential ($V_p = 1.5-2.5$ V). This potential is higher than that in the molecular gases as is the electron temperature ($T_e = 1-1.5$ eV); see Fig. 9. Higher electron temperature during the discharge is reasonable, since argon has no excited states below 11.5 eV. Hence, plasma cooling is slower relative to the cooling rate in molecular gases. Even higher electron temperatures are expected in pure argon than those measured here. Moreover, since recombination is not a viable decay mechanism for Ar^+ (given that it is a three-body process), the discharge should be diffusion dominated. Thus the plasma should show a slowly decaying afterglow but instead shows rapid quenching of plasma species as in the molecular gas case. In the Plexiglas chamber, this rapid quenching was attributed to the poor base pressure, which resulted in 5%–10% of the plasma operating pressure being air. In the aluminum chamber, the base pressure was at least 2 orders of magnitude better and yet similar results were seen. This result is surprising until we look at the plasma fluxes as seen by the mass spectrometer during and after the *e*-beam. Once the *e*-beam source is off, we see that the dominant ion quickly becomes H_2O^+. The trace amounts of H_2O in the high vacuum environment were still enough (and the cross section large enough) to charge exchange the Ar^+ to H_2O^+ very rapidly. See Ref. 7 for additional treatments of this and other mass spectrometry measurements in *e*-beam produced plasmas.

VI. SUMMARY

We have used electron beam produced plasmas in molecular and noble gases resulting in plasma densities in $1-5 \times 10^{11}$ cm^{-3} in conducting (aluminum) and insulating (Plexiglas) vessels as measured by Langmuir probes and microwave transmission. While completely different probe techniques were used in each system, the discharge characteristics were transferable across chambers. probe contamination issues are very different but were quantified and discussed in detail. A two-temperature fitting routine showed primary electron temperatures in these discharges were 0.3–0.5 eV for the molecular gasses and ~1.2 eV for argon. Due to the *e*-beam ionization mechanism, nontraditional heating of the plasma electrons can result in extremely non-Maxwellian distributions. The consistently low (1–3 V) plasma potentials, however, demonstrate that the electron temperature must be low as well, regardless of the distribution. Mass spectrometry shows relative ion species in an oxygen discharge to be $2(O^+):1(O_2^+)$ and predominantly Ar^+ in an argon discharge, at operating pressures of 40–100 mTorr.

VII. CONCLUSION

The strong similarities in the molecular and noble gas discharges show that *e*-beam ionization is fairly independent of background gas. Unlike typical ICP or glow discharges, electron temperatures are low because there is no external heating and the plasma electrons are simply byproducts of the *e*-beam collisions. Standard Langmuir probe techniques can be employed, although at these operating pressures and conditions, contamination issues can seriously affect information collected from such probes.

ACKNOWLEDGMENTS

The authors greatly appreciate insightful conversations with Dr. Martin Lampe and Dr. Wally Manheimer. NRL/NRC postdoctoral research associates. S.G.W. and D.D.B. gratefully acknowledge support from the National Research Council. This work was supported by the Office of Naval Research.

[1] R. F. Fernsler, W. M. Manheimer, R. A. Meger, J. Mathew, D. P. Murphy, R. E. Pechacek, and J. A. Gregor, Phys. Plasmas **5**, 2137 (1998); V. Burdovitsin and E. Oks, Rev. Sci. Instrum. **70**, 2975 (1999); W. M. Manheimer, R. F. Fernsler, M. Lampe, and R. A. Meger, Plasma Sources Sci. Technol. **9**, 370 (2000).

[2] M. A. Kushner, W. Z. Collison, and D. N. Ruzic, J. Vac. Sci. Technol. A **14**, 2094 (1996); K. D. Schatz and D. N. Ruzic, Plasma Sources Sci. Technol. **2**, 100 (1993).

[3] From R. F. Fernsler *et al.* in Ref. 1, a 2 kV electron beam loses ~3 eV/cm @30 mTorr, thus a 2.5 keV beam in 100 mTorr has a range of 1.4 m, much shorter than the dimensions of our chamber.

[4] M. C. Myers, D. D. Hinshelwood, R. A. Meger, and R. E. Pechacek, Proceedings of the 12th IEEE Pulsed Power Conference, Monterey, CA 1999.

[5] W. E. Amatucci, M. E. Koepke, T. E. Sheridan, M. J. Alport, and J. J. Carroll III, Rev. Sci. Instrum. **64**, 1253 (1993).

[6] It was necessary to use the same 10 mil tungsten wire in the emissive probe to get a more rugged filament for our operating conditions.

[7] S. G. Walton *et al.*, J. Vac. Sci. Technol. A (these proceedings).

[8] Electron beam current is considered to be the current collected at the beam dump anode. This may be an overestimate.

[9] For a thin plasma sheet, the evanescent wave can get through the sheet if the sheet thickness <microwave wavelength. Basic result is a factor of 2 increase in n (cm^{-3}) from the simple equation $n(\text{cm}^{-3}) = 1.23 \times 10^{12} \times [f(\text{GHz})/10]^2$. D. P. Murphy, R. F. Fernsler, and R. A. Merger, NRL Internal Report No. NRL/MR/6754--99-8368, May 1999 (unpublished).

[10]A single temperature version of this algorithm is discussed by J. J. Carroll III, M. E. Koepke, W. E. Amatucci, T. E. Sheridan, and M. J. Alport, Rev. Sci. Instrum. **65**, 2991 (1994).
[11]Attempts to derive the energy distribution function from the probe data taken in these experiments proved to be noninformative, as the data smoothing required completely overshadowed the underlying physical information. We have been implementing a 12-bit resolution data acquisition system to circumvent this problem. See D. D. Blackwell *et al.*, J. Vac. Sci. Technol. A (these proceedings).
[12]We saw no evidence of significant negative ion densities during or after the *e*-beam pulse as characterized by a symmetric probe *I–V* trace. The fact that we have cold plasma electrons would imply that the electron attachment mechanism is non-negligible. However, for the most electronegative gas studied here, oxygen, the attachment cross section is extremely low at these electron energies. (See D. Rapp and D. D. Briglia, J. Chem. Phys. **43**, 1480 (1965).
[13]F. J. Mehr and M. A. Biondi, Phys. Rev. **181**, 264 (1969).
[14]P. M. Mul and J. W. McGowan, J. Phys. B **12**, 1591 (1979).